

# The Influence of Disulfide, Thioacetal and Lanthionine-Bridges on the Conformation of a Macrocyclic Peptide

William T. P. Darling,<sup>[a]</sup> Lianne H. E. Wieske,<sup>[b]</sup> Declan T. Cook,<sup>[a]</sup> Abil E. Aliev,<sup>[a]</sup> Laurent Caron,<sup>[c]</sup> Emily J. Humphrys,<sup>[c]</sup> Angelo Miguel Figueiredo,<sup>[d]</sup> D. Flemming Hansen,<sup>[d]</sup> Máté Erdélyi,<sup>\*[b]</sup> and Alethea B. Tabor<sup>\*[a]</sup>

Cyclisation of peptides by forming thioether (lanthionine), disulfide (cystine) or methylene thioacetal bridges between side chains is established as an important tool to stabilise a given structure, enhance metabolic stability and optimise both potency and selectivity. However, a systematic comparative study of the effects of differing bridging modalities on peptide conformation has not previously been carried out. In this paper, we have used the NMR deconvolution algorithm, NAMFIS, to determine the conformational ensembles, in aqueous solution,

of three cyclic analogues of angiotensin(1–7), incorporating either disulfide, or non-reducible thioether or methylene thioacetal bridges. We demonstrate that the major solution conformations are conserved between the different bridged peptides, but the distribution of conformations differs appreciably. This suggests that subtle differences in ring size and bridging structure can be exploited to fine-tune the conformational properties of cyclic peptides, which may modulate their bioactivities.

## Introduction

Beyond rule-of-five (bRo5) macrocycles (500–5000 Da) are a major focus of interest in medicinal chemistry and chemical biology.<sup>[1,2]</sup> They have the potential to occupy conformational space that cannot be covered by traditional small molecule drugs and probes, and thus can address undruggable targets such as protein-protein interactions.<sup>[3,4]</sup> Cyclic peptides are an important class of bRo5 macrocycles,<sup>[5,6]</sup> particularly cystine-bridged peptides, which can be designed from naturally occurring bioactive peptide sequences and are readily synthesised. Cyclising bioactive peptides by forming disulfide bonds frequently stabilises the structure, increases potency and selectivity, enhances stability to proteases and can also lead to increased membrane permeability.<sup>[7,8]</sup> However, such disulfide

bridges can be easily reduced or scrambled, which limits the *in vivo* stability of these peptides.<sup>[9,10]</sup>

To further improve the metabolic stability and retain the potency and selectivity of cystine-bridged peptides, both thioacetal and thioether (lanthionine)-bridged analogues have been explored. A simple protocol for the rebridging of disulfides by the insertion of a methylene group to form a stable thioacetal has recently been reported<sup>[11]</sup> and has been used to prepare biologically active analogues of peptides with increased serum stability.<sup>[11,12]</sup> The first thioether-bridged analogue of a medically relevant peptide was reported in 1997 by Goodman and co-workers, who prepared lanthionine-bridged somatostatin analogues which had greater receptor binding selectivity and a longer half-life *in vivo* than cystine-bridged peptides.<sup>[13]</sup> Since then, lanthionine analogues of several other classes of biologically active peptides have been prepared and shown to be highly potent, receptor-selective and resistant to proteolysis.<sup>[14–20]</sup> However, in a few cases, this cyclisation modality resulted in the peptide analogues having reduced or no binding to the target receptor.<sup>[21,22]</sup> Excitingly, a thioether stabilised angiotensin(1–7) analogue, cAng(1–7) exhibits significantly enhanced vasodilation and plasma stability compared with the naturally occurring linear peptide.<sup>[23]</sup> cAng(1–7) can be delivered orally and via the lung<sup>[24]</sup> and a variant sequence with a *D*-Lys at the N-terminus, LP2, has completed preclinical and in-human safety studies for treatment of cardiovascular disease<sup>[25]</sup> and colorectal cancer.<sup>[26]</sup> Solid-phase synthesis of lanthionine-bridged peptides using orthogonally protected lanthionine monomers has been established<sup>[27,28]</sup> with monomers corresponding to all possible lanthionine diastereoisomers being available.<sup>[27,29]</sup> In a complementary approach, the post-translational modification enzymes have been exploited for the biosynthesis of engineered lanthionine-type therapeutic peptides.<sup>[30–32]</sup> They have also been used to generate phage display libraries<sup>[19]</sup> and lanthipeptide libraries<sup>[20]</sup> in *E. coli*.

[a] W. T. P. Darling, D. T. Cook, A. E. Aliev, A. B. Tabor  
Department of Chemistry, University College London, 20, Gordon Street,  
London WC1H 0AJ, UK  
E-mail: a.b.tabor@ucl.ac.uk

[b] L. H. E. Wieske, M. Erdélyi  
Department of Chemistry-BMC, Uppsala University, SE-751 23 Uppsala,  
Sweden  
E-mail: mate.erdelyi@kemi.uu.se

[c] L. Caron, E. J. Humphrys  
Biosynth Laboratories Ltd (formerly Cambridge Research Biochemicals Ltd),  
17-18 Belasis Court, Belasis Hall Technology Park, Billingham TS23 4AZ, UK

[d] A. M. Figueiredo, D. F. Hansen  
Department of Structural and Molecular Biology, Division of Biosciences,  
University College London, UCL Darwin Building, Gower Street, London  
WC1E 6BT UK

Supporting information for this article is available on the WWW under  
<https://doi.org/10.1002/chem.202401654>

© 2024 The Authors. Chemistry - A European Journal published by Wiley-VCH GmbH. This is an open access article under the terms of the Creative Commons Attribution License, which permits use, distribution and reproduction in any medium, provided the original work is properly cited.

However, what is currently lacking is a molecular level understanding of the effect that these three different bridging modalities - disulfide, methylene thioacetal and thioether - have on the underlying conformational properties of the resulting cyclic peptides, for instance as shown in Figure 1. Replacement of disulfide bonds will cause changes in polarity, hydrophobicity, bond length and bond angles, properties which are typically consistent and well characterised across cystine bridges. These bond length/angles and polarity deviations can cause global conformational changes or peptide-target polarity mismatches which can prove either detrimental, or beneficial, for biological activity and target selectivity.<sup>[33]</sup> Moreover, macrocycles are conformationally flexible. This allows them to adapt to give high-affinity binding to a variety of targets, and can also confer solubility in both aqueous and non-polar environments resulting in enhanced cell permeability.<sup>[1–6]</sup> Understanding the structures of the individual conformers that make up the solution ensemble is vital to understanding these medically desirable properties.<sup>[34–36]</sup> Despite this, there have been virtually no studies comparing the effects of different cyclisation modal-

ities on the solution conformation of these peptides. Conformational analyses by NMR of disulfide and lanthionine-bridged sandostatin analogues<sup>[37]</sup> and of disulfide- and lanthionine-bridged peptides binding to death receptor 5<sup>[19]</sup> have been reported. In these studies, similar conformations with the backbone atoms overlaying closely were seen for both pairs of peptide analogues, however only a single average conformation was reported for each peptide.

Deriving a single time-averaged structure from NMR leads to an unrealistic structure for flexible systems. Time-averaged structures are heavily skewed towards the shortest found distances. This is because NOE intensity is proportional to the inverse of the sixth power of the distance ( $r^{-6}$ ) between two nuclei and is most accurate for short distances ( $<2.5$  Å) due to non-linear scaling of NOE-derived interproton distances. Instead, NMR data is best interpreted by a set of rapidly interconverting conformations giving rise to a single set of time-averaged signals. A solution to this problem is to use an NMR deconvolution algorithm. For example, NAMFIS (NMR Analysis of Molecular Flexibility In Solution)<sup>[38]</sup> deconvolutes the individual conformers that make up the time-averaged set of signals observed in the NMR spectra into its constituent conformers and their molar fractions.<sup>[39]</sup> We have previously applied this to the analysis of macrocyclic peptides<sup>[36,40,41]</sup> including the bicyclic *N*-terminus of the lantibiotic nisin, which has both a lanthionine and a methyl lanthionine bridge.<sup>[42]</sup>

In this paper, we have used NAMFIS to determine the solution ensemble of three macrocyclic peptides. These are analogues of cAng(1–7) which differ only by the presence of a lanthionine (thioether), disulfide or methylene thioacetal bridge. This has allowed us for the first time to compare the effects of these three modes of side-chain peptide bridging on the conformations of the peptides in solution.

## Results and Discussion

### Design and Synthesis of the Cyclic Angiotensin(1–7) Analogues

Due to the increased *in vivo* stability and enhanced vasodilatory effect of cAng(1–7) compared with angiotensin(1–7), we used cAng(1–7) as a model system for this study (Figure 1). This peptide has a relatively small macrocyclic ring (12-membered ring formed from four amino acid residues bridged by a thioether) but still has potent GPCR agonist activity.<sup>[23]</sup> No conformational analysis of this peptide has previously been carried out and none of its bioactive, target-bound or unbound structures were known. In the original report,<sup>[23]</sup> cAng(1–7) 1 was produced using bacteria expressing the relevant enzymes for post-translational modification of peptides to give lanthionine bridges. This results in (*S*)-stereochemistry at residue 4 and (*R*)-stereochemistry at residue 7. Although the related analogue, LP2, is the first lanthipeptide GPCR agonist to pass stage 1 clinical trials, the additional *N*-terminal *D*-Lys residue was added to provide protection against aminopeptidases and does not alter the receptor binding properties.<sup>[25]</sup> Moreover, only the

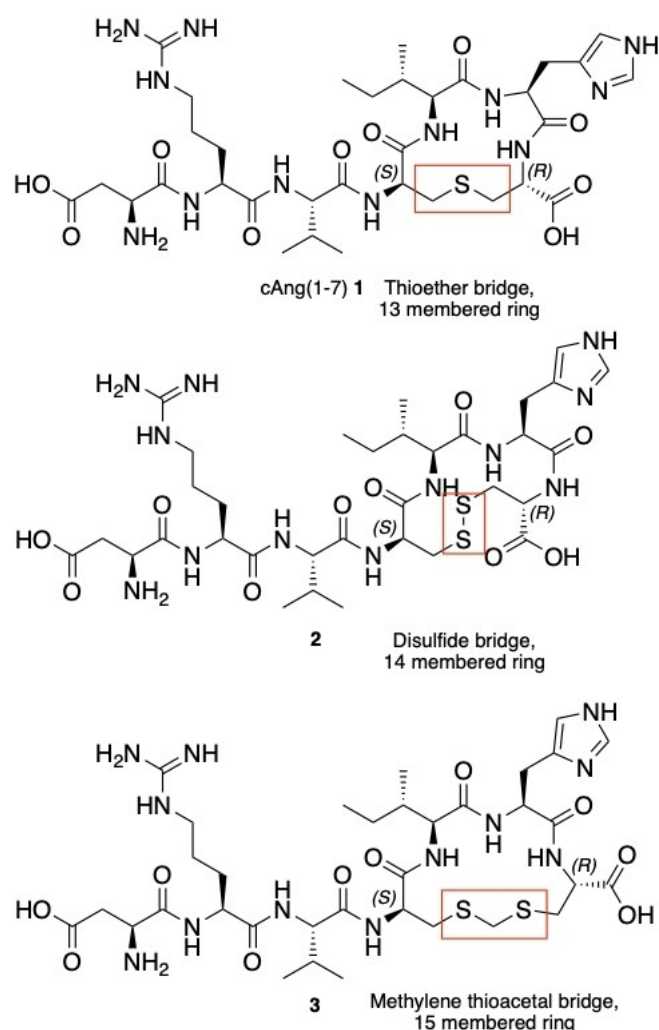


**Figure 1.** Macroyclic peptides with the sequence <sup>1</sup>Asp-<sup>2</sup>Arg-<sup>3</sup>Val-c-[<sup>D</sup><sup>4</sup>Xaa-<sup>5</sup>Ile-<sup>6</sup>His-<sup>7</sup>Xaa]: cAng(1–7) 1 (lanthionine bridge) 2 (disulfide bridge) and 3 (methylene thioacetal bridge).

residues involved in the macrocycle would be subject to analysis with NAMFIS, as the more flexible parts of the peptide such as the *N*-terminal tail are unlikely to adopt rigid or well-defined conformations and are less likely to be fully sampled by conformational searches.

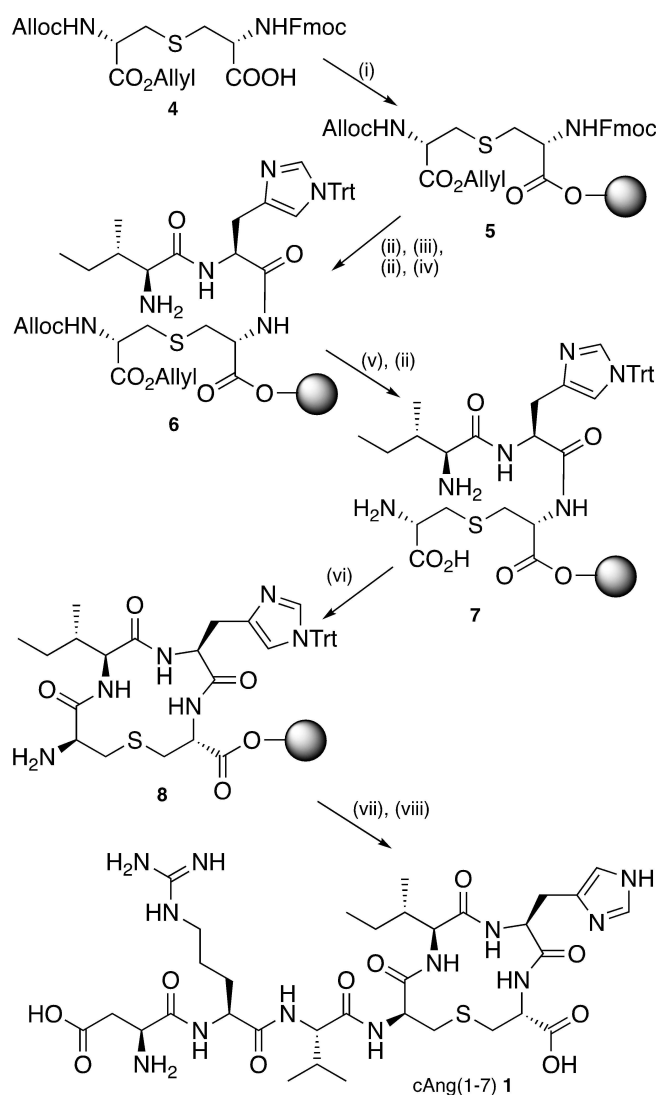
To examine the effects of expanding the bridge, we designed the novel peptide analogues **2** (disulfide bridged) and **3** (methylene thioacetal bridged). In order to preserve the <sup>4</sup>Xaa(S) and <sup>7</sup>Xaa(R) stereochemistry in the analogues, we included *D*-Cys at residue 4 in peptides **2** and **3** (Figure 1). As these two peptides were previously unreported, receptor binding and/or bioactivity data are not available. However, this series of peptides were chosen as a model system for investigating the effect of increasing bridge size and different bridge composition on conformational ensembles of cyclic peptides. We synthesised cAng(1–7) **1** using the solid-phase peptide synthesis (SPPS) methodology that we and others have previously developed and used for lantibiotic synthesis (Scheme 1).<sup>[42–48]</sup> Orthogonally protected (Alloc, allyl/Fmoc) lanthionine **4** was prepared using a modification of previously published routes<sup>[46,48]</sup> (Supporting Information) and added to 2-chlorotrityl chloride (CTC) resin to afford **5**. The trityl resin was used, as it has previously been shown to be effective in suppressing racemisation which can often occur when Cys is the first residue.<sup>[49]</sup> Standard SPPS was then used to form the resin-bound linear peptide **6**. Selective removal of the allyl and Alloc protecting groups,<sup>[45]</sup> followed by Fmoc deprotection, gave **7**. This was then cyclised on-resin using HOAt, PyAOP and DIPEA<sup>[50]</sup> to afford **8**. Standard SPPS to install residues 1–3 was followed by resin cleavage and side chain deprotection to give **1** in 25% yield.

Peptide **2** was synthesised using standard SPPS methods and the linear peptide was oxidised with I<sub>2</sub> to afford the disulfide-bridged peptide in 28% overall yield. The crude linear peptide intermediate was also directly converted to the methylene thioacetal analogue **3**, employing a preliminary treatment with TCEP followed by bridging with CH<sub>2</sub>I<sub>2</sub> (Scheme 2) to afford **3** in 8% overall yield.

### NAMFIS Analysis

All three peptides were highly soluble in water. The NMR experiments were carried out in 9:1 H<sub>2</sub>O:D<sub>2</sub>O mixtures, as cAng(1–7) (and LP2) are GPCR agonists and therefore act extracellularly. The peptides were isolated after HPLC purification as their trifluoroacetic acid salts and the pH of the peptides was not adjusted. The NMR experiments were thus carried out at pH ranging between 3 and 4 in which the <sup>2</sup>Arg and <sup>6</sup>His side chains and the terminal –NH<sub>2</sub> group were all protonated, and the <sup>1</sup>Asp and C-terminal –COOH groups deprotonated.

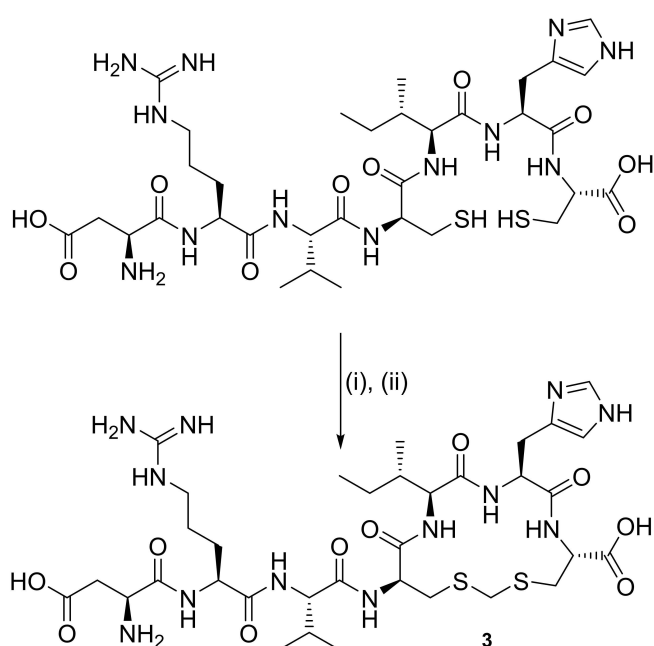
NAMFIS uses NOE-derived interproton distances and <sup>3</sup>J<sub>HH</sub> scalar coupling constants to find the best fit solution between a population weighted combination of theoretical conformations and experimentally determined distances and coupling constants from the NMR derived data.<sup>[38,39]</sup> Figure 2 summarises the inter-residue distances and <sup>3</sup>J<sub>NH-αH</sub> couplings that were used in



**Scheme 1. Reagents and Conditions:** (i) 2-chlorotrityl resin, DIPEA, CH<sub>2</sub>Cl<sub>2</sub> (ii) Fmoc deprotection with 40%, then 20%, piperidine in DMF (iii) Fmoc-His(Trt)-OH, DIC, HOBT·xH<sub>2</sub>O, DIPEA, DMF (iv) Fmoc-Ile-OH, HATU, DIPEA, DMF (v) Pd(PPh<sub>3</sub>)<sub>4</sub>, phenylsilane, CH<sub>2</sub>Cl<sub>2</sub> (vi) HOAt, PyAOP, DIPEA, DMF (vii) SPPS of remaining amino acids (Fmoc-Val-OH, Fmoc-Arg(Pbf)-OH, Fmoc-Asp(OtBu)-OH) (viii) TFA, TIPS, H<sub>2</sub>O.

the NAMFIS analyses for each peptide. A full list of interproton distances is given in the Supporting Information (Tables S7–S9). H<sub>2</sub>O:D<sub>2</sub>O mixtures allowed for the examination of backbone amide protons, however the use of solvent suppression obscured and altered the integrals of the α protons nearby the suppressed solvent signal. Interproton distances for the α protons were instead determined in D<sub>2</sub>O with EASY ROESY without solvent suppression in the instance where insufficient NOEs were present in the NOESY spectra for structural analysis.

All the peptide bonds were orientated in the lower-energy *trans* configuration prior to Monte Carlo Multiple Minima (MCM) simulations<sup>[51,52]</sup> as the orientation of the peptide bonds are not inverted from *trans* to *cis* during the calculations. In linear peptides which do not have Pro or *N*-alkylated residues, the amide bonds are almost exclusively (> 99.9%)



Scheme 2. Reagents and Conditions: (i) TCEP.HCl, Na<sub>2</sub>CO<sub>3</sub> (ii) CH<sub>2</sub>I<sub>2</sub>, Et<sub>3</sub>N.

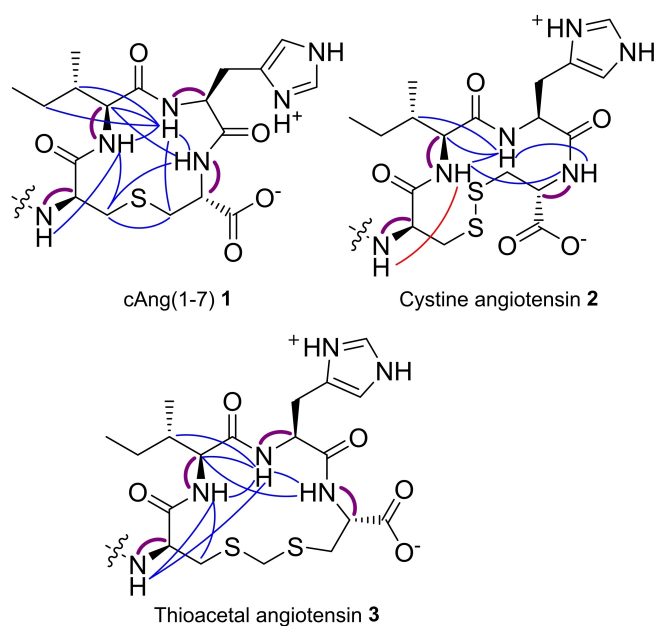


Figure 2. Inter-residue interproton distances (blue lines) and scalar couplings (purple lines) used in the NAMFIS analyses. The red line indicates an interproton distance that when removed during validation causes an 18% change in the solution ensemble of peptide 2.

*trans*.<sup>[53,54]</sup> This is also observed in both linear and small to medium-sized cyclic peptides, including disulfide-bridged peptides.<sup>[55]</sup> As conversion from *trans* to *cis* isomers is slow on the NMR timescale, any cyclic peptides containing *cis* amide bonds would be observed as a distinct set of NMR signals<sup>[55–57]</sup> instead of within the time-averaged set of signals that was subject to NAMFIS analysis. Hence it is not necessary to sample the conformational space of peptides containing *cis* peptide

bonds.<sup>[58]</sup> Unless stated otherwise, all heavy atoms within the macrocycle backbone in addition to the amide nitrogen at residue 4 were used for pairwise RMSD comparisons.

The stereotopic assignments of diastereotopic protons were determined by finding the best fit between the back-calculated and experimentally-derived interproton distances and coupling constants following NAMFIS analysis of each stereotopic assignment. For stereotopic assignments that resulted in identical RMSD values, the assignment that resulted in the least degree of overfitting was chosen.

Within the NMR spectra for cAng(1–7) 1 and disulfide-bridged peptide 2, the diastereotopic β-proton signals of <sup>4</sup>Lan and <sup>7</sup>Cys, respectively, were overlapping. In previous work, overlapped NOEs could not be used to determine accurate distances as it is unknown how much of each separate NOE contributes to the overlapped signal. However, we have found that it is possible to account for these overlapped NOEs, as the observed intensities are the sum of the NOEs to each of the overlapping protons. This overlap can be accounted for within the theoretical ensemble by averaging the distances to the two overlapping protons according to Equation (1):

$$r_{(AB)Z} = (r_{AZ}^{-6} + r_{BZ}^{-6})^{\frac{1}{6}} \quad (1)$$

where  $r_{AZ}$  and  $r_{BZ}$  are the distances derived from the theoretical ensemble between proton H<sub>Z</sub> with the overlapping protons H<sub>A</sub> and H<sub>B</sub> respectively, and  $r_{(AB)Z}$  is the ‘combined distance’. This ‘combined distance’ equates to the interproton distance derived from overlapping NOEs. Due to the inverse sixth power relationship between NOE build-up rates and interproton distances, the observed distance of two overlapping protons is shorter than either component distance. Using this approach, we have been able to add additional NOE-derived interproton distances from overlapping signals that could not be resolved, thus significantly improving the reliability of the NAMFIS analysis.

### Solution Ensembles

The solution ensembles of all three peptides are strikingly similar, despite the different bridge length and accordingly different bridge geometries (Figure 3). For each of the peptides, two major conformational families, **A** and **B**, are observed (Figure 3). In family **A**, the <sup>4</sup>Xaa NH is oriented towards the macrocyclic R groups, whereas in family **B** the <sup>4</sup>Xaa NH is oriented away from the macrocyclic R groups. The overall orientation of the acyclic N-terminal residues (<sup>1</sup>Asp-<sup>2</sup>Arg-<sup>3</sup>Val) is thus dependent on the <sup>4</sup>Xaa NH orientation. There are two sub-populations of the family **A** conformers, **A1** and **A2**, which are highly conserved between all three peptides and which differ only by the orientation of the amide bonds between the <sup>5</sup>Ile and <sup>6</sup>His residues, and a less well-defined <sup>7</sup>Xaa carboxylic acid position for **A2** likely due to the shortage of inter-residue interproton distances from this residue (Figure 2). The backbone of peptides 1, 2 and 3 overlay almost exactly in conformations **A1** and **A2**, with low pairwise RMSD range between each of the

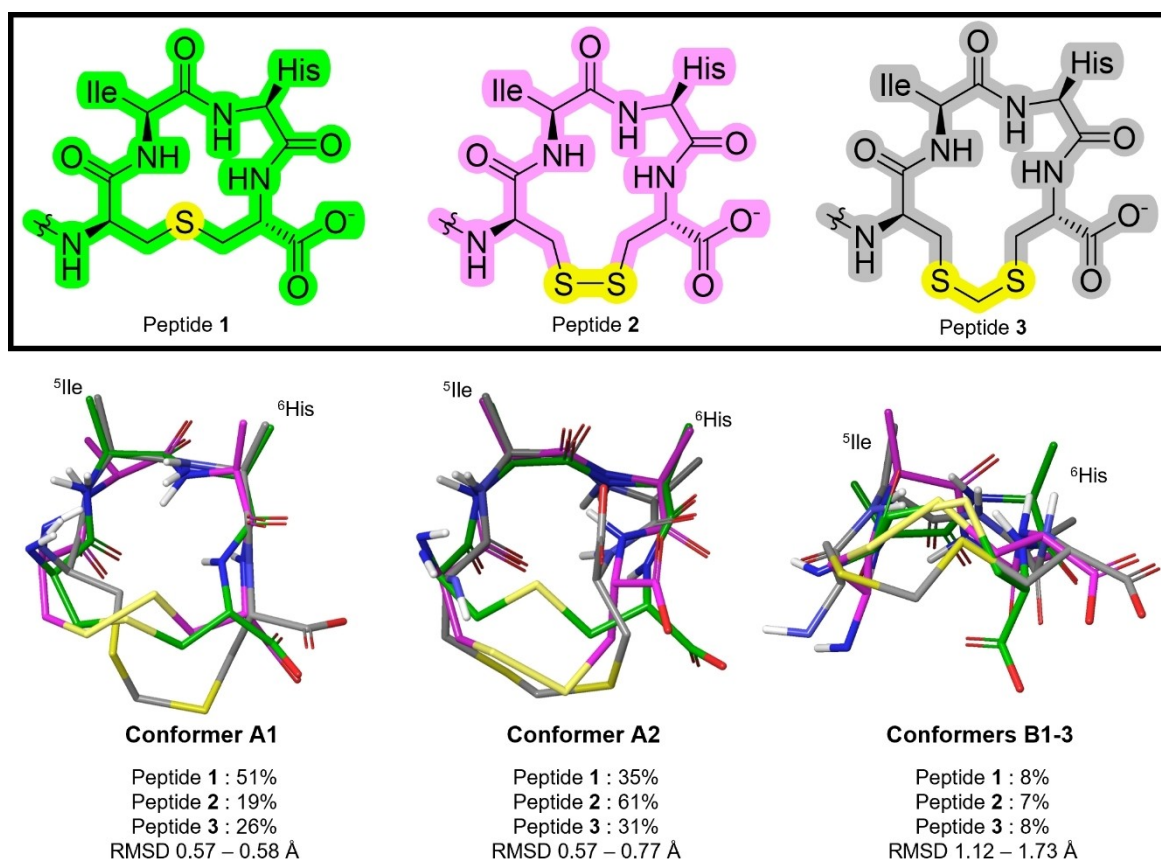


**Figure 3.** Major conformational families adopted by macrocyclic peptides 1, 2 and 3. The peptide backbones are overlaid and the spread of RMSD of the backbones is given for each of the conformational families.

three peptides (0.57–0.77 Å). The principal variations in the macrocycle conformations are between the lanthionine/disulfide/methylene thioacetal bridges. However, the distribution of sub-conformers varies with the ring size and bridging structure. The lanthionine bridged cAng(1–7) peptide 1 is biased towards conformation A1, whereas the disulfide bridged peptide 2 favours conformation A2. The methylene thioacetal bridged peptide adopts similar amounts of the two conformations.

In contrast, the population of family B conformers is small (less than 10%) and the percentage that adopt the B family of conformations is consistent irrespective of ring size (Supporting Information, Figures S4–S7). As the ring size increases, a small number of minor conformations related to the A family are also observed for peptides 2 and 3 which vary only by the orientation of backbone amides. These minor conformers however appear at low abundances (8–15%) (Supporting Information, Figures S5 and S6). Conformers with abundances below 5% were not considered further as these might in the worst cases be fitting artefacts. Due to the insufficient number of interproton distances to the <sup>7</sup>Xaa αH, from which the position of the carboxylate group is inferred, the position of the C-terminal –COOH is uncertain, even within the same conformational family. It is also worth noting that no interproton distances to the <sup>4</sup>Xaa αH could be determined due to the use of solvent suppression. Interproton distances to this α-proton

could have given more confidence in determining the populations of families A and B with <sup>4</sup>Xaa NH oriented towards and away from the macrocyclic R groups, respectively. For the NAMFIS analysis of peptide 2, EASY ROESY spectra in neat D<sub>2</sub>O without water suppression were also acquired to determine interproton distances to the <sup>4</sup>Cys α-proton. The EASY ROESY and NOESY data were then combined. Despite this, the removal of the only inter-residue interproton distance to <sup>4</sup>Cys caused significant (18%) changes in the solution ensemble. This is however expected in regions of low information.<sup>[58]</sup>

The NAMFIS analysis of all three peptides incorporated the peptide backbone of residues c[D<sup>4</sup>Xaa-<sup>5</sup>Ile-<sup>6</sup>His-<sup>7</sup>Xaa]. All the β-carbons of these four residues were additionally incorporated, allowing us to be confident of the overall orientation of the side chains. For cAng(1–7) 1, the analysis also successfully incorporated the entire flexible <sup>5</sup>Ile side chain. However, for peptides 2 and 3, the flexible side chains of <sup>5</sup>Ile and <sup>6</sup>His had to be omitted, and thus the position of these R groups can therefore only be characterised as far as the β-carbons. It is a common procedure to neglect the analysis of flexible side chains at the determination of macrocycle conformations, in order to avoid the risk of contaminating the calculations with uncertain data of flexible regions that are cumbersome or impossible to properly sample computationally.<sup>[42,59]</sup> For peptide 3, despite numerous interproton distances to the methylene

thioacetal CH<sub>2</sub> group, a valid NAMFIS result could not be obtained when incorporating the methylene interproton distances. This is likely due to the inability to fully sample all of the possible conformations in the theoretical ensemble for this part of the peptide, suggesting that the thioacetal bridge is highly flexible and adopts many conformations. Attempts to sample this conformational space were made with additional MCMM calculations while fixing torsion angles of the macrocyclic backbone into conformations already determined from preliminary NAMFIS analyses. However, this larger theoretical ensemble still failed to produce a valid solution ensemble. Due to this, interproton distances to the methylene thioacetal CH<sub>2</sub> group were not used in the NAMFIS analysis and the position of the methylene thioacetal bridge is not accurately defined in the solution ensemble. However, overall we have a reliable analysis of the conformations of the macrocyclic core of this potent GPCR agonist (and analogues **2** and **3**) and the orientations of the <sup>5</sup>Ile and <sup>6</sup>His sidechains. We predict that this is likely to represent the part of the molecule that is of relevance to the receptor binding.<sup>[41,42]</sup>

## Conclusions

In order to compare the effects on the conformational preferences of peptides that have been cyclised via structurally similar side-chain bridges, we have synthesised three cyclic angiotensin(1–7) analogues incorporating either a cystine bridge, or non-reducible lanthionine or methylene thioacetal bridges. We have determined the solution ensembles of the macrocyclic core of these three peptides by using the NMR deconvolution algorithm NAMFIS. For each peptide, two distinct classes of conformers (**A** and **B**) arise from the orientation of the <sup>4</sup>Xaa residue, resulting in distinct directions of the *N*-terminal tail. For all three peptides, the about 90% of the solution ensembles adopt family **A** conformations in which the <sup>4</sup>Xaa NH is oriented towards the macrocyclic R groups, and the remaining 10% orientated away from the macrocyclic R groups (family **B**). Within this family, there are two sub-populations (**A1**, **A2**) which are conserved between all three peptides, however the populations of each can differ by around 30% as the ring size changes. As the macrocycle ring size increases, the number of conformations present in solution also increases, an indication of an increased flexibility. These conformational changes, however, are relatively small in most instances, primarily being the orientation of the backbone amides. Despite being only small changes, it is interesting to observe that these amide bond orientation changes are less frequent in the smaller macrocycles. Because the proportion of these family **B** conformations does not change across the series, it can be inferred that the small differences in the size of the macrocycle do not have a significant impact on global conformational changes beyond the macrocycle.

In the system studied here, both thioether and methylene thioacetal bonds are demonstrated to be suitable non-reducible isosteric replacements for disulfide bonds that do not significantly change the macrocycle or global peptide conformation.

The differing distributions of conformations between the major **A1** and **A2** conformers suggests that thioether, disulfide and methylene thioacetal linkages can be used to fine-tune affinity for a desired biological target, by alteration of the populations of conformers. As no structural data is currently available for the cAng(1–7)-receptor interaction, or for analogues **2** and **3**, these results will be particularly important and will inform future structural and pharmacology studies. Even if the major solution conformer may not correspond to the biologically active conformation,<sup>[34,42]</sup> the protein-bound conformation of low-molecular-weight ligands is generally presumed to be represented to a measurable extent in the ensemble of conformations for the compound free in solution.<sup>[60–63]</sup> A binding induced major conformational change requiring large energy investment is unlikely.

For cAng(1–7) we have demonstrated that the three cyclisation modalities cannot be regarded as completely interchangeable. The peptides encompassing different cyclisation modalities have different distributions of conformations within the same broad conformational ensemble. In addition, we have extended the scope of NAMFIS analysis by developing an approach to derive interproton distances where NOE signals overlap. This significantly improves the accuracy of the analysis.

Understanding the conformational preferences of flexible macrocycles, including cyclic peptides, is vital to predict their bioactivity. The conformations of a peptidic macrocycle will depend on the macrocycle size, side-chains and local environment. Whereas it is not possible to provide general rules for all types of cyclic peptides based on the three model systems examined herein, we envisage that the powerful approach presented in this paper will allow the investigation of further examples. This will provide extensive datasets that can be used to parameterise future molecular dynamic simulations and provide training sets for machine learning approaches. Currently, conventional molecular dynamics (MD) simulation methods are unable to identify relevant solution conformations and tend to get trapped in a large number of local minima.<sup>[64]</sup> This is in part because these methods have been developed and tested on limited datasets that derive from solid state or ensemble average structures,<sup>[34]</sup> and partly because the energy difference between the conformations is frequently rather small. Combining data from experimentally determined ensembles with MD simulations with enhanced sampling techniques and improved force fields,<sup>[65]</sup> medicinal chemists will finally be able to realise the elusive goal of prediction, design and synthesis of conformationally constrained peptides which are exquisitely fine-tuned to occupy the desired conformational space for potent biological activity. The recent publication of bRo5 cyclic peptides incorporating other types of thioether linkages<sup>[66,67]</sup> or different cyclisation modalities<sup>[68–70]</sup> with nanomolar target affinities, high stability, membrane permeability and oral availability has further emphasised the critical importance of understanding their solution ensembles, and we envisage that the lessons learned from this study of three key cyclisation modalities will ultimately be applicable to all bRo5 macrocycles.

## Materials and Methods

Experimental procedures and characterisation data for the synthesis of (Alloc, allyl/Fmoc) (2*S*, 6*R*)-lanthionine **4** and peptides **1**, **2** and **3** are given in the ESI. The complete experimentally determined NMR data, <sup>1</sup>H and <sup>13</sup>C assignments of the peptides, information about the theoretical conformational ensembles and the output ensembles (including tables of the interproton distances and coupling constants) for the three peptides are also presented in the Supporting Information (Tables S1–S23, Figures S4–S7).

### NMR Spectroscopy

For the assignment and NAMFIS analyses, <sup>1</sup>H, <sup>13</sup>C, COSY, TOCSY, HSQC, HMBC and NOESY spectra were recorded in a 9:1 mixture of H<sub>2</sub>O:D<sub>2</sub>O at 25 °C using excitation sculpting water suppression pulse programmes (using standard Bruker sequences, noesyegpph). Additional EASY ROESY<sup>[71]</sup> spectra were obtained for peptide **2** in D<sub>2</sub>O without solvent suppression. 1.5 mg of each peptide were dissolved in 0.6 mL of solvent. All spectra of peptides **1** and **2** were acquired on a 900 MHz Bruker Avance III HD spectrometer equipped with a 5 mm TCI cryogenic probe, except for the EASY ROESY spectra which were acquired on a 500 MHz Bruker Avance NEO equipped with a 5 mm TXO cryogenic probe. NOESY spectra of peptide **3** were acquired on an 800 MHz Bruker Avance III HD equipped with a TCI cryogenic probe and <sup>1</sup>H, <sup>13</sup>C, COSY, TOCSY, HSQC and HMBC were acquired on a 700 MHz Bruker Avance NEO. Seven NOESY spectra were acquired for each peptide with mixing times from 100–700 ms (100 ms increments). For peptides **1** and **2** each NOESY spectrum was recorded with a relaxation delay of 2.5 s, 16 scans, 2048 points in the direct dimension and 512 in the indirect dimension, and a spectral window of 10 ppm. For peptide **3**, each NOESY spectrum was recorded with a relaxation delay of 3.0 s, 16 scans, 1536 points in the direct dimension and 512 in the indirect dimension, and a spectral window of 10 ppm. Seven EASY ROESY spectra for peptide **2** were recorded with mixing times 50–350 ms (50 ms increments), each recorded with a relaxation delay of 2.5 s, 16 scans, 2048 points in the direct dimension and 512 in the indirect dimension, and a spectral window of 10 ppm.

Interproton distances were generated from NOE build-up curves from a series of NOESY and EASY ROESY spectra using the initial rate approximation<sup>[72]</sup> and using two geminal methylene protons (1.78 Å) as a reference.<sup>[73]</sup> Interproton distances were thus calculated according to Equation (2):

$$r_{AB} = r_{ref} \times \left( \frac{\sigma_{ref}}{\sigma_{AB}} \right)^{\frac{1}{6}} \quad (2)$$

where  $r_{AB}$  is the interproton distance between protons HA and HB in Ångström,  $r_{ref}$  is 1.78 Å, and  $\sigma_{ref}$  and  $\sigma_{AB}$  are the gradient of the build-up curve for the reference pair and proton pair of interest, respectively.

Cross-peak intensities were normalised to diagonal peak intensity by applying “peak amplitude normalisation for improved cross-relaxation” (PANIC)<sup>[72,74]</sup> (Equation 3):

$$I_{norm} = \left( \frac{cross\ peak_{AB} \times cross\ peak_{BA}}{diagonal\ peak_A \times diagonal\ peak_B} \right)^{0.5} \quad (3)$$

In most instances, only proton-pairs with at least five mixing times that gave rise to a linear NOE build-up curve ( $R^2 \geq 0.95$ ) were used for distance calculations.

<sup>3</sup>J<sub>NH-OH</sub> were measured directly from the amide signals in <sup>1</sup>H spectra. Overlapping NOE signals were integrated in their entirety to give rise to combined interproton distances which were used in the NAMFIS analyses.

### Conformational Sampling

A total of six MCMM conformational searches were performed for peptide **2**, eight for peptide **1** and fourteen for peptide **3** to create the theoretical input ensembles. All conformational searches were set-up using MacroModel as implemented within the Schrödinger suite.<sup>[51,52]</sup> A combination of implicit solvent systems (water and chloroform)<sup>[75]</sup> and different force-fields (OPL4, OPLS 2005, MMFF and AMBER\*) were performed for each peptide with a high energy cut-off to ensure sampling of the entire conformational space. The MCMM searches were performed using 100,000 steps with the energy window for saving compounds 42 kJ/mol, a minimum RMSD difference for saving compounds of 0.5 Å and the Polak-Ribiere type conjugate gradient (PRCG) with a maximum of 5000 iteration steps for the energy minimization. These conditions were to maximise the number of different conformers and decrease the risk of real conformers not being sampled within the theoretical ensemble rather than providing a realistic ensemble for any particular solvent system. Additional MCMM searches for peptide **3** while fixing torsion angles within the macrocyclic backbone to those found within preliminary NAMFIS analyses were conducted to better sample the conformational space. The results of conformational searches performed with the four different force fields and two solvent models each, for each peptide were combined and redundant conformers were eliminated. This was done by comparison of all heavy atoms within the macrocycle (<sup>4</sup>Xaa to <sup>7</sup>Xaa) for peptide **1** and all heavy atoms until the β carbons for peptides **2** and **3** using an RMSD cut-off between 0.9 and 1.1 Å. The combined and reduced ensemble originating from the 8 Monte Carlo conformational searches were used as input for the NAMFIS analyses.

### NAMFIS Analyses

The version of NAMFIS used, and instructions for installation, are available at the open access repository Zenodo with DOI:10.5281/zenodo.6866837.<sup>[38,39]</sup> The conformational ensembles of peptides **1**, **2** and **3** were determined using the NAMFIS algorithm by fitting the back-calculated interproton distances and coupling constants from the conformations in the computer-generated theoretical ensembles to those determined experimentally, following previous work.<sup>[38,39]</sup>

$J$  couplings were given a flat error of  $\pm 1$  Hz,<sup>[39,76]</sup> whereas interproton distances were given an error proportional to their length as described by Nevins *et al.*,<sup>[77]</sup> whereby longer distances are given larger errors. Distances were grouped in ranges of 0.5 Å (<2.50, 2.50–2.99, 3.00–3.49, >3.49) and each group given incrementally increased errors ( $\pm 0.3$ –1.2 Å).<sup>[38,77]</sup>

Theoretical distances to methyl groups were averaged according to Equation (4):

$$r_{X,Me} = \left( \frac{r_{AX}^{-6} + r_{BX}^{-6} + r_{CX}^{-6}}{3} \right)^{-\frac{1}{6}} \quad (4)$$

where  $r_{AX}$ – $r_{CX}$  are the interproton distance between each proton of the methyl group to the proton of interest H<sub>X</sub>.

The theoretical distance arising from an overlapping pair of NOE signals were calculated according to Equation (1). Scalar couplings

of the theoretical ensemble conformers were back-calculated using the following modified Karplus equation for  $^3J_{\text{NH}-\alpha\text{H}}$  couplings<sup>[76, 78, 79]</sup> (Equation 5):

$$^3J_{\text{NH}-\alpha\text{H}} = 9.4 \cos(\theta)^2 - 1.1 \cos(\theta) + 0.4 \quad (5)$$

Conformations of each peptide were clustered based on similar backbone RMSD values ( $< 0.80 \text{ \AA}$ ). The most populated of each of these conformers within a cluster were then used as the representative structure when used to compare the conformers between the different peptide analogues. Conformations between peptides were considered the same if the representative structure of each cluster had pairwise RMSD values below  $0.80 \text{ \AA}$ .

Populations obtained by NAMFIS analyses were validated by the removal of each data point in turn, by the addition or subtraction of up to 5% random noise to the experimental data to simulate the expected experimental error of interproton distances of 3–7%,<sup>[39,72]</sup> and by comparison of the experimental data to the NAMFIS back-calculated values. NAMFIS solutions that did not change by more than 10% during the validation process were considered valid. An exception was made for the disulfide bridged analogue **2** which varied by 18% during validation when a single interproton distance was removed in an area of the peptide with few distance restraints. NAMFIS has been shown to unlikely detect conformers of 5% or less, and have a maximum accuracy of around  $\pm 9\%$ .<sup>[39]</sup> For these reasons, conformers with populations of 5% or less were not considered, as these may be mathematical artefacts of the fitting process.

For each peptide the flexible *N*-terminus ( $^1\text{Asp}$ – $^3\text{Val}$ ) was too flexible to incorporate into the NAMFIS analysis. Likewise, for peptides **2** and **3** the side chains of the macrocyclic residues ( $^4\text{Cys}$  to  $^7\text{Cys}$ ) beyond the  $\beta$ -carbons were too flexible to incorporate into the NAMFIS analysis. For peptide **1** the entire  $^5\text{Ile}$  side-chain was successfully incorporated into the NAMFIS analysis but not the  $^6\text{His}$  side-chain beyond the  $\beta$ -carbon.

## Supporting Information Summary

The original NMR spectroscopic data (FIDs) of each peptide; NMRReDATA of each peptide;<sup>[80,81]</sup> theoretical ensemble of conformers; and the solution ensembles of each peptide, are available at Zenodo: DOI:10.5281/zenodo.11073289. The authors have cited additional references within the Supporting Information.<sup>[82–85]</sup>

## Acknowledgements

We would like to thank the BBSRC LIDo PhD programme (BB/M009513/1) and Biosynth Laboratories Ltd (formerly Cambridge Research Biochemicals Ltd) for an iCASE PhD studentship to W.T.P.D.. D.T.C. was supported by a PhD studentship funded by UCL Division of Biosciences. D.F.H. acknowledges the UKRI and EPSRC for financial support (EP/X036782/1). We also thank the Wenner-Gren Foundations for a Guest Researcher Stipend to A.B.T. We are grateful to the Swedish Research Council for financial support (2020-03431). This study made use of the NMR Uppsala infrastructure, which is funded by the Department of Chemistry-BMC and the Disciplinary Domain of Medicine and

Pharmacy. We are grateful for access to the 900 MHz NMR instruments at the Swedish NMR Centre in Gothenburg. The BBSRC (BB/R000255/1), Wellcome Trust (ref.101569/z/13/z), and the EPSRC (EP/X036782/1) are also acknowledged for supporting the NMR facility at University College London. The computations were enabled by resources provided by the National Academic Infrastructure for Supercomputing in Sweden (NAISS) and the Swedish National Infrastructure for Computing (SNIC) at Tetralith, partially funded by the Swedish Research Council through grant agreements no. 2022-06725 and no. 2018-05973, under project numbers 2025/5-431 and 2023/5-392.

## Conflict of Interests

The authors declare no conflict of interest.

## Data Availability Statement

The data that support the findings of this study are openly available in Zenodo at 10.5281/zenodo.11073289, reference number 11073289.

**Keywords:** Conformation · Cyclic peptide · Lanthionine · NAMFIS · NMR spectroscopy

- [1] B. C. Doak, B. Over, F. Giordanetto, J. Kihlberg, *Chem. Biol.* **2014**, *21*, 1115–1142.
- [2] D. G. Jimenez, V. Poongavanam, J. Kihlberg, *J. Med. Chem.* **2023**, *66*, 5377–5396.
- [3] B. C. Doak, J. Zheng, D. Dobritzsch, J. Kihlberg, *J. Med. Chem.* **2016**, *59*, 2312–2327.
- [4] E. Valeur, S. M. Guéret, H. Adihou, R. Gopalakrishnan, M. Lemurell, H. Waldmann, T. N. Grossmann, A. T. Plowright, *Angew. Chem. Int. Ed.* **2017**, *56*, 10295–10323.
- [5] M. R. Naylor, A. T. Bockus, M.-J. Blanco, R. S. Lokey, *Curr. Opin. Chem. Biol.* **2017**, *38*, 141–147.
- [6] H. Zhang, S. Chen, *RSC Chem. Biol.* **2022**, *3*, 18–31.
- [7] R. Tugyi, G. Mezö, E. Fellingner, D. Andreu, F. Hudecz, *J. Pept. Sci.* **2005**, *11*, 642–649.
- [8] M. Góngora-Benítez, J. Tulla-Puche, F. Albericio, *Chem. Rev.* **2014**, *114*, 901–926.
- [9] M. A. Hossain, J. D. Wade, *Acc. Chem. Res.* **2017**, *50*, 2116–2127.
- [10] M. Muttenthaler, A. Andersson, A. D. de Araujo, Z. Dekan, R. J. Lewis, P. F. Alewood, *J. Med. Chem.* **2010**, *53*, 8585–8596.
- [11] C. M. B. Kourra, N. Cramer, *Chem. Sci.* **2016**, *7*, 7007–7012.
- [12] N. Zheng, S. B. Christensen, C. Dowell, L. Purushottam, J. J. Skalicky, J. M. McIntosh, D. H.-C. Chou, *J. Med. Chem.* **2021**, *64*, 9513–9524.
- [13] G. Ósapay, L. Prokai, H.-S. Kim, K. F. Medzihradsky, D. H. Coy, G. Liapakis, T. Reisine, G. Melacini, Q. Zhu, S. H.-H. Wang, R.-H. Mattern, M. Goodman, *J. Med. Chem.* **1997**, *40*, 2241–2251.
- [14] Y. Rew, S. Malkmus, C. Svensson, T. L. Yaksh, N. N. Chung, P. W. Schiller, J. A. Cassel, R. N. DeHaven, M. Goodman, *J. Med. Chem.* **2002**, *45*, 3746–3754.
- [15] H. Li, X. Jiang, S. B. Howell, M. Goodman, *J. Pept. Sci.* **2000**, *6*, 26–35.
- [16] H. Li, X. Jiang, M. Goodman, *J. Pept. Sci.* **2001**, *7*, 82–91.
- [17] A. Kelleman, R.-H. Mattern, M. D. Pierschbacher, M. Goodman, *Biopolymers (Pept. Sci.)* **2003**, *71*, 686–695.
- [18] R. Rink, A. Arkema-Meter, I. Baudoin, E. Post, A. Kuipers, S. A. Nelemans, M. H. J. Akanbi, G. N. Moll, *J. Pharmacol. Toxicol. Methods* **2010**, *61*, 210–218.

- [19] J. H. Urban, M. A. Moosmeier, T. Aumüller, M. Thein, T. Bosma, R. Rink, K. Groth, M. Zully, K. Siegers, K. Tissot, G. N. Moll, J. Prassler, *Nat. Commun.* **2017**, *8*, 1500.
- [20] X. Yang, K. R. Lennard, C. He, M. A. Walker, A. T. Ball, C. Doigneaux, A. Tavassoli, W. A. van der Donk, *Nat. Chem. Biol.* **2018**, *14*, 375–380.
- [21] K. Pulka-Ziac, V. Pavet, N. Chekkat, K. Estieu-Gionnet, R. Rohac, M.-C. Lechner, C. R. Smulski, G. Zeder-Lutz, D. Altschuh, H. Gronemeyer, S. Fournel, B. Odaert, G. Guichard, *ChemBioChem* **2015**, *16*, 293–301.
- [22] M. Muttenthaler, A. Andersson, A. D. de Araujo, Z. Dekan, R. J. Lewis, P. F. Alewood, *J. Med. Chem.* **2010**, *53*, 8585–8596.
- [23] L. D. Kluskens, S. A. Nelemans, R. Rink, L. de Vries, A. Meter-Arkema, Y. Wang, T. Walther, A. Kuipers, G. N. Moll, M. Haas, *J. Pharmacol. Exp. Ther.* **2009**, *328*, 849–854.
- [24] L. de Vries, C. E. Reitzema-Klein, A. Meter-Arkema, A. van Dam, R. Rink, G. N. Moll, M. H. J. Akanbi, *Peptides* **2010**, *31*, 893–898.
- [25] P. Namsolleck, A. Richardson, G. N. Moll, A. Mescheder, *Peptides* **2021**, *136*, 170468.
- [26] P. Namsolleck, L. de Vries, G. N. Moll, *Peptides* **2023**, *160*, 170920.
- [27] A. Tabor, *Org. Biomol. Chem.* **2011**, *9*, 7606–7628.
- [28] A. Tabor, *Bioorg. Chem.* **2014**, *55*, 39–50.
- [29] T. Denoël, C. Lemaire, A. Luxen, *Chem. – Eur. J.* **2018**, *24*, 15421–15441.
- [30] L. D. Kluskens, A. Kuipers, R. Rink, E. de Boef, S. Fekken, A. J. Driessen, O. P. Kuipers, G. N. Moll, *Biochemistry* **2005**, *44*, 12827–12834.
- [31] Y. Shi, X. Yang, N. Garg, W. A. van der Donk, *J. Am. Chem. Soc.* **2011**, *133*, 2338–2341.
- [32] G. N. Moll, A. Kuipers, R. Rink, T. Bosma, L. de Vries, P. Namsolleck, *Biochem. Soc. Trans.* **2020**, *48*, 2195–2203.
- [33] A. Gori, P. Gagni, S. Rinaldi, *Chem. – Eur. J.* **2017**, *23*, 14987–14995.
- [34] E. Danelius, V. Poongavanam, S. Peintner, L. H. E. Wieske, M. Erdélyi, J. Kihlberg, *Chem. – Eur. J.* **2020**, *26*, 5231–5244.
- [35] F. Begnini, V. Poongavanam, Y. Atilaw, M. Erdélyi, S. Schiesser, J. Kihlberg, *ACS Med. Chem. Lett.* **2021**, *12*, 983–990.
- [36] J. Bogaerts, Y. Atilaw, S. Peintner, R. Aerts, J. Kihlberg, C. Johannessen, M. Erdélyi, *RSC Adv.* **2021**, *11*, 4200–4208.
- [37] G. Melacini, Q. Zhu, G. Ösapay, M. Goodman, *J. Med. Chem.* **1997**, *40*, 2252–2258.
- [38] D. O. Cicero, G. Barbato, R. Bazzo, *J. Am. Chem. Soc.* **1995**, *117*, 1027–1033.
- [39] L. H. E. Wieske, S. Peintner, M. Erdélyi, *Nat. Rev. Chem.* **2023**, *7*, 511–524.
- [40] E. Danelius, U. Brath, M. Erdélyi, *Synlett* **2013**, *24*, 2407–2410.
- [41] E. Danelius, M. Pettersson, M. Bred, J. Min, M. B. Waddell, R. K. Guy, M. Grotli, M. Erdélyi, *Org. Biomol. Chem.* **2016**, *14*, 10386–10393.
- [42] R. Dickman, E. Danelius, S. A. Mitchell, D. F. Hansen, M. Erdélyi, A. B. Tabor, *Chem. – Eur. J.* **2019**, *25*, 14572–14582.
- [43] S. Bregant, A. B. Tabor, *J. Org. Chem.* **2005**, *70*, 2430–2438.
- [44] B. Mothia, A. N. Appleyard, S. Wadman, A. B. Tabor, *Org. Lett.* **2011**, *13*, 4216–4219.
- [45] R. Dickman, S. A. Mitchell, A. M. Figueiredo, D. F. Hansen, A. B. Tabor, *J. Org. Chem.* **2019**, *84*, 11493–11512.
- [46] Z. V. F. Wright, S. McCarthy, R. Dickman, F. E. Reyes, S. Sanchez-Martinez, A. Cryar, I. Kilford, A. Hall, A. K. Takle, M. Topf, T. Gonen, K. Thalassinou, A. B. Tabor, *J. Am. Chem. Soc.* **2017**, *139*, 13063–13075.
- [47] W. Liu, A. S. H. Chan, H. Liu, S. A. Cochran, J. C. Vederas, *J. Am. Chem. Soc.* **2011**, *133*, 14216–14219.
- [48] A. C. Ross, H. Liu, V. R. Pattabiraman, J. C. Vederas, *J. Am. Chem. Soc.* **2010**, *132*, 462–463.
- [49] Y. Fujiwara, K. Akaji, Y. Kiso, *Chem. Pharm. Bull.* **1994**, *42*, 724–726.
- [50] F. Albericio, M. Cases, J. Alsina, S. A. Triolo, L. A. Carpino, S. A. Kates, *Tetrahedron Lett.* **1997**, *38*, 4853–4856.
- [51] F. Mohamadi, N. G. Richard, W. C. Guida, R. Liskamp, M. Lipton, C. Cauffman, G. Chang, T. Hendrickson, W. C. Still, *J. Comput. Chem.* **1990**, *11*, 440–467.
- [52] Schrödinger Release 2023-1: MacroModel, Schrödinger, LLC, New York, NY, **2023**.
- [53] G. Fischer, *Chem. Soc. Rev.* **2000**, *29*, 119–127.
- [54] J. Zhang, M. W. Germann, *Biopolymers* **2011**, *95*, 755–762.
- [55] K. Nguyen, M. Iskandar, D. L. Rabenstein, *J. Phys. Chem. B* **2010**, *114*, 3387–3392.
- [56] M. J. Deetz, J. E. Fahey, B. D. Smith, *J. Phys. Org. Chem.* **2001**, *14*, 463–467.
- [57] B. S. Thakkar, J.-S. M. Svendsen, R. A. Engh, *J. Phys. Chem. A* **2017**, *121*, 6830–6837.
- [58] L. H. E. Wieske, Y. Atilaw, V. Poongavanam, M. Erdélyi, J. Kihlberg, *Chem. – Eur. J.* **2023**, *29*, e202202798.
- [59] E. Danelius, H. Andersson, P. Jarvoll, K. Lood, J. Gräfenstein, M. Erdélyi, *Biochemistry* **2017**, *56*, 3265–3272.
- [60] D. Altschuh, O. Vix, B. Rees, J. C. Thierry, *Science* **1992**, *256*, 92–94.
- [61] R. M. Wenger, J. France, G. Bovermann, L. Walliser, A. Widmer, H. Widmer, *FEBS Lett.* **1994**, *340*, 255–259.
- [62] J. Jimenez-Barbero, A. Canales, P. T. Northcote, R. M. Buey, J. M. Andreu, J. F. Diaz, *J. Am. Chem. Soc.* **2006**, *128*, 8757–8765.
- [63] P. Thepchatr, T. Eliseo, D. O. Cicero, D. Myles, J. P. Snyder, *J. Am. Chem. Soc.* **2007**, *129*, 3127–3134.
- [64] C. Peng, Y. Atilaw, J. Wang, Z. Xu, V. Poongavanam, J. Shi, J. Kihlberg, W. Zhu, M. Erdélyi, *ACS Omega* **2019**, *4*, 22245–22250.
- [65] J. Damjanovic, J. Miao, H. Huang, Y.-S. Lin, *Chem. Rev.* **2021**, *121*, 2292–2324.
- [66] M. L. Merz, S. Habeshian, B. Li, J.-A. G. L. David, A. L. Nielsen, X. Ji, K. Il Khwily, M. J. Duany Benitez, P. Phothisirath, C. Heinis, *Nat. Chem. Biol.* **2024**, *20*, 624–633.
- [67] J. H. Faris, E. Adaligil, N. Popovych, S. Ono, M. Takahashi, H. Nguyen, E. Plise, J. Taechalertpaisarn, H.-W. Lee, M. F. T. Koehler, C. N. Cunningham, R. S. Loker, *J. Am. Chem. Soc.* **2024**, *146*, 4582–4591.
- [68] S. Habeshian, M. L. Merz, G. Sangouard, G. K. Mothukuri, M. Schüttel, Z. Bognár, C. Diaz-Perlas, J. Vesin, J. B. Chapalay, G. Turcatti, L. Cendron, A. Angelini, C. Heinis, *Nat. Commun.* **2022**, *13*, 3823.
- [69] T. J. Tucker, M. W. Embrey, C. Alleyne, R. P. Amin, A. Bass, B. Bhatt, E. Bianchi, D. Branca, T. Bueters, N. Buist, S. N. Ha, M. Hafey, H. He, J. Higgins, D. G. Johns, A. D. Kerekes, K. A. Koepflinger, J. T. Kueth, N. Li, B. Murphy, P. Orth, S. Salowe, A. Shahripour, R. Tracy, W. Wang, C. Wu, Y. Xiong, H. J. Zokian, H. B. Wood, A. Walji, *J. Med. Chem.* **2021**, *64*, 16770–16800.
- [70] M. Tanada, M. Tamiya, A. Matsuo, A. Chiyoda, K. Takano, T. Ito, M. Irie, T. Kotake, R. Takeyama, H. Kawada, R. Hayashi, S. Ishikawa, K. Nomura, N. Furuichi, Y. Morita, M. Kage, S. Hashimoto, K. Nii, H. Sase, K. Ohara, A. Ohta, S. Kuramoto, Y. Nishimura, H. Iikura, T. Shiraishi, *J. Am. Chem. Soc.* **2023**, *145*, 16610–16620.
- [71] C. M. Thiele, K. Petzold, J. Schleuchner, *Chem. – Eur. J.* **2009**, *15*, 585–588.
- [72] S. Macura, B. T. Farmer, L. R. Brown, *J. Magn. Reson.* **1986**, *70*, 493–499.
- [73] C. P. Butts, C. R. Jones, E. C. Towers, J. L. Flynn, L. Appleby, N. J. Barron, *Org. Biomol. Chem.* **2011**, *9*, 177–184.
- [74] H. T. Hu, K. Krishnamurthy, *J. Magn. Res.* **2006**, *182*, 173–177.
- [75] W. C. Still, A. Tempczyk, R. C. Hawley, T. Hendrickson, *J. Am. Chem. Soc.* **1990**, *112*, 6127–6129.
- [76] C. A. G. Haasnoot, F. A. A. M. de Leeuw, C. Altona, *Tetrahedron* **1980**, *36*, 2783–2792.
- [77] N. Nevins, D. Cicero, J. P. Snyder, *J. Org. Chem.* **1999**, *64*, 3979–3986.
- [78] M. Karplus, *J. Chem. Phys.* **1959**, *30*, 11–15.
- [79] P. Schmieder, H. Kessler, *Biopolymers* **1992**, *32*, 435–440.
- [80] S. Kuhn, L. H. E. Wieske, P. Trevorow, D. Schober, N. E. Schlörer, J. M. Nuzillard, P. Kessler, J. Junker, A. Herráez, C. Farès, M. Erdélyi, M. Jeannerat, *Magn. Reson. Chem.* **2021**, *59*, 792–803.
- [81] M. Pupier, J. M. Nuzillard, J. Wist, N. E. Schlörer, S. Kuhn, M. Erdélyi, C. Steinbeck, A. J. Williams, C. Butts, T. D. W. Claridge, B. Mikhova, W. Robien, H. Dashti, H. R. Eghbalnia, C. Farès, C. Adam, P. Kessler, F. Moriaud, M. Elyashberg, D. Argyropoulos, M. Pérez, P. Giraudeau, R. R. Gil, P. Trevorow, D. Jeannerat, *Magn. Reson. Chem.* **2018**, *56*, 703–715.
- [82] M. F. Mohd Mustapa, R. Harris, N. Bulic-Subanovic, S. L. Elliott, S. Bregant, M. F. A. Groussier, J. Mould, D. Schultz, N. A. L. Chubb, P. R. J. Gaffney, P. C. Driscoll, A. B. Tabor, *J. Org. Chem.* **2003**, *68*, 8185–8192.
- [83] K. Manzor, K. Ó Proinsias, F. Kelleher, *Tetrahedron Lett.* **2017**, *58*, 2959–2963.
- [84] O. Al Musaimi, A. Basso, B. G. De La Torre, F. Albericio, *ACS Comb. Sci.* **2019**, *21*, 717–721.
- [85] C. R. Jones, C. P. Butts, J. N. Harvey, *Beilstein J. Org. Chem.* **2011**, *7*, 145–150.

Manuscript received: April 26, 2024

Accepted manuscript online: July 2, 2024

Version of record online: August 20, 2024